An Unexpected Atropisomerically Stable 1,1-Biphenyl at Ambient Temperature in Solution, Elucidated by Vibrational Circular Dichroism (VCD)

by **Teresa B. Freedman*** [a]), **Xiaolin Cao** [a]), **Laurence A. Nafie*** [a]), **Monica Kalbermatter** [b]), **Anthony Linden** [b]), and **Andreas Johannes Rippert*** [b])

[a]) Department of Chemistry, 1-014 Center for Science and Technology, Syracuse University, Syracuse, New York 13244-4100, USA

[b]) Organisch-Chemisches Institut der Universität Zürich, Winterthurerstr. 190, CH-8057 Zürich

Biphenyls with only two substituents at the '*peri*'-position normally show rotation about their chiral axis at room temperature. Using vibrational circular dichroism (VCD), we found no evidence for rotation of (*P*)-2′-[(4*S*)-4,5-dihydro-4-(1-methylethyl)oxazol-2-yl][1,1′-biphenyl]-2-methanol ((*P*,*S*)-**1**) in $CDCl_3$ about its chiral axis due to stabilization by intramolecular H-bonding. All rotamers of **1** were calculated at the DFT level, and, from these optimized structures, the VCD spectra were calculated and compared to the measured VCD spectra. The best agreement between calculated and measured spectra is obtained when two rotamers are present in solution. These rotamers differ primarily in their intramolecular H-bonding interactions, having either OH ··· N (the form present in the solid state) or OH ··· O H-bonds, *i.e.*, a rotation of the heterocycle in **1** takes place in solution.

1. Introduction. – The synthesis of enantiomerically pure molecules is one of the leading challenges in organic synthesis in academic as well as industrial research. These highly valuable compounds are used as building blocks for natural-product synthesis, as well as as auxiliaries and ligands in transition-metal catalysis for the asymmetric synthesis of potent pharmaceuticals and highly active agrochemicals.

We are mainly interested in molecules that possess a chiral axis and that belong to the class of atropisomers, *e.g.*, 1,1′-biphenyls. If at least two substituents are located at the 2,2′, 3,3′, 5,5′ or 6,6′ positions of each of the aromatic rings of the 1,1′-biphenyl moiety, two rotational isomers can be drawn that behave as enantiomers. However, when only two substituents are located at the '*peri*' positions, the 1,1′-biphenyl moiety is in most cases not rotationally stable at room temperature, and racemization takes place [1–5] (*cf. Scheme 1*). The activation energy (E_A) for the rotation about the chiral axis (racemization or atropisomerization) is >20 kcal/mol for an optically stable 1,1′-biphenyl. It is best to use atropisomerism if further chiral centers are located in the substituents attached at the biphenyl moiety, to distinguish the rotation around the axis from any changes at the chiral centers.

The stabilization of such rotational processes can be achieved by different approaches. One is the buttressing effect of substituents in the 3,3′ or 5,5′ positions with sterically demanding groups such as the I-atom, *e.g.*, 2,2′,3,3′-tetraiodo[1,1′-biphenyl]-5,5′-dicarboxylic acid, which has a measured E_A (rac) of 28.1 kcal/mol [3] compared with 21.8 kcal/mol for 2,2′-diiodo[1,1′-biphenyl]5,5′-dicarboxylic acid [3]. The latter compound, because of the sterically demanding iodo substituents in the '*peri*'

Scheme 1. *Equilibrium at Room Temperature of 2,2′-Disubstituted 1,1′-Biphenyls*

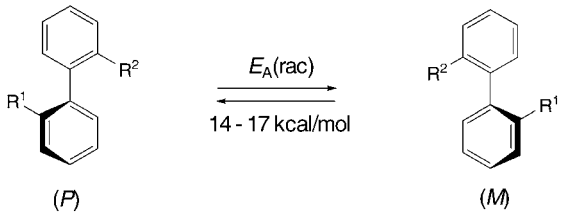

positions, is one of the rare examples of enantiomerically stable compounds with only two *o*-substituents in the biphenyl moiety [6]. Another, elegant approach is to diminish the rotational stability of highly substituted biaryls by introducing small bridges (up to two atoms) between two '*peri*' substituents, as shown by *Bringmann et al.* [7][8]. This bridge forces the angle between the planes of the two benzene rings of the 1,1′-biphenyl moiety to be *ca.* 30–40° (the least steric strain occurs at around 90°) and lowers the E_A (rac) below 20 kcal/mol [4][5][9]. As soon as the bridge has more than four atoms, the opposite trend for the E_A (rac) is found [4][5]. An alternate, flexible approach is to introduce a stabilizing H-bonded bridge between the two '*peri*' substituents attached at the biphenyl moiety. The stability in solution can be increased or diminished by changing the solvent, which offers an interesting opportunity for the planning of high-yield, asymmetric organic syntheses. However, determining such a dynamic process by means of electronic CD or NMR measurements for diastereoisomers can be very complicated and difficult to interpret. Vibrational circular dichroism (VCD), the differential interaction of left- and right-circularly polarized IR radiation during vibrational excitation, has emerged as a powerful technique for elucidating the solution structures of chiral molecules [10–12], including recent studies of molecules with chiral axes [13][14]. The approach involves comparison of experimental IR and VCD spectra with calculations carried out at the DFT level for conformers of a specific configuration of the molecule. Since the solution conformations do not interchange on the vibrational timescale, VCD features can be used to identify both the absolute configuration and the solution conformation.

2. Results and Discussion. – We are interested in the synthesis of substituted 1,1′-biphenyls without C_2 symmetry as versatile ligands for asymmetric transition-metal catalysis. These compounds are synthetically accessible by ring opening of racemic [1,1′-biphenyl]-2,2′-dicarboxylic anhydrides with N-nucleophiles, such as optically pure amino alcohols, to yield the desired 2′-[(2-hydroxyethyl)carbamoyl][1,1′-biphenyl]-2-carboxylic acids (*Scheme 2*). The detailed synthesis will be published in a subsequent paper [15].

This method was used to synthesize 2′-[(*S*)-4,5-dihydro-4-(1-methylethyl)oxazol-2-yl]-1,1′-biphenyl]-2-methanol **1** in four steps starting from racemic [1,1′-biphenyl]-2,2′-dicarboxylic anhydride and (*S*)-valinol. After purification by column chromatography, **1** was isolated as a white solid, and a sample was recrystallized from ^{t}BuOMe/hexane to yield colorless crystals suitable for an X-ray crystal-structure analysis. The result is shown in *Fig. 1*.

Scheme 2

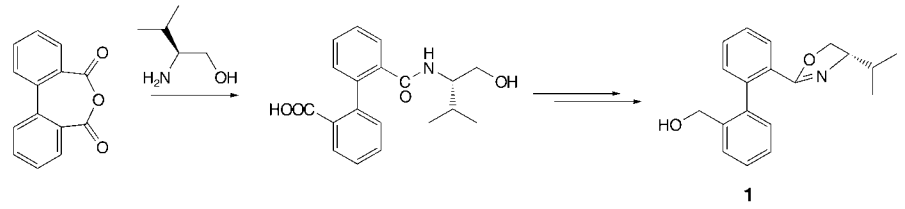

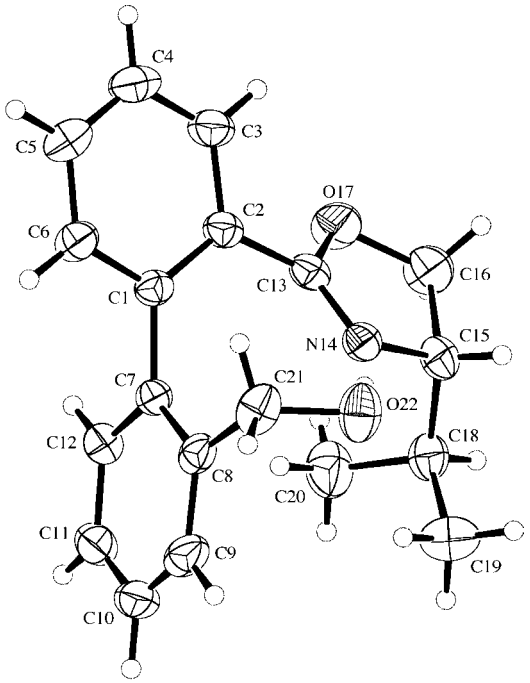

Fig. 1. *Molecular structure of* (P)*-2′-[(4*S*)-4,5-dihydro-4-(1-methylethyl)oxazol-2-yl][1,1′-biphenyl]-2-methanol ((*P,S*)-***1***)*. Arbitrary numbering.

The measured crystal contained both the enantiomerically and diastereoisomerically pure (*P*,*S*)-**1**. In this case, where (*S*)-valinol was used as the enantiomerically pure amino alcohol, the two diastereoisomers (*P*,*S*)- and (*M*,*S*)-**1** can be expected. These diastereoisomers should be in equilibrium in solution at room temperature (*cf.* 1,1′-biphenyls with two '*peri*' substituents). As a result of the X-ray crystal-structure analysis, it was found that an OH···N H-bond is present in the molecule, with a H···N distance of 1.87(2) Å, an O···N distance of 2.845(2) Å, and an OH···N angle of 175(2)°. This H-bond is also facilitated by the arrangement of the two benzene rings of the biphenyl backbone, which are virtually perpendicular to one another with the angle between the planes of the benzene rings being 89.00(8)°. A further small stabilizing effect on the conformation of the molecule could also come from the isopropyl substituent. One of the Me groups sits over the plane of one of the benzene rings of the

biphenyl moiety with a H···Ph(centroid) distance of 3.18 Å and a H···Ph(centroid) angle of 165°, which means that a binding interaction takes place. However, in solution the E_A for the rotation of this isopropyl group is expected to be small.

Analytical measurements, such as electronic CD and dynamic NMR, gave no clear result for the presence of pure (*P*,*S*)-**1** as two rotamers, showing no rotation around the chiral axis. The ^{1}H-NMR measurements in $CDCl_3$ showed that crude and solid **1**, as well as crystalline **1** and the residue of the mother liquor, all gave the same spectra, which showed two rotamers. To distinguish the two observed rotamers, we performed low-temperature ^{1}H-NMR measurements (as low as −40°; the crystals from the X-ray crystal-structure analysis were dissolved at this low temperature-in $CDCl_3$). However, even at this temperature, we observed two rotamers with similar chemical shifts to those observed at room temperature, and the small differences in the chemical shifts can be explained simply by temperature effects. Upon heating this solution to room temperature, a spectrum was obtained which was identical to that of **1** when no cooling had been used. Rotation around the chiral axis in **1** has an estimated energy barrier, E_A, of 14 to 17 kcal/mol, so only a slow rotation, if any, should take place at −40° (*cf. Scheme 1)*. Therefore, NMR measurements do not readily allow assignment of the dynamic process for the observed two rotamers, and no comparison with the solid structure can be drawn.

To determine whether the crystallization led to a single stereoisomer (as distinct from spontaneous separation of the two possible (*P*,*S*)- and (*M*,*S*)-stereoisomers upon crystallization) and whether the H-bond can also stabilize this stereoisomer in aprotic nonpolar solvents, VCD measurements were carried out in the solid state as well as in $CDCl_3$ solution. In addition to the mentioned determination of the absolute configuration at the chiral biphenyl axis and the stability of the H-bond by VCD, this new chiral measurement method could be useful for clarifying the dynamic process in solution (structural assignment of the two rotamers).

For the solution measurements, a solution (*ca.* 10 mg sample/ 50 µl $CDCl_3$) prepared in a coldroom at 5° was placed in a demountable cell with CaF_2 windows and transferred to a temperature-control unit while maintaining the low temperature during the transfers. IR and VCD spectra were measured for 1 h each at 5°, 10°, 15°, and 20°. The sample was then held at room temperature (23°) overnight, and the room-temperature spectra were subsequently recorded. This procedure was repeated for the $CDCl_3$ solvent, and solvent baselines were employed for the spectra displayed in *Figs. 2* and *3*. The VCD spectra exhibit a high noise level at 1660 cm^{-1} due to the large absorbance (>1) at that frequency (*Fig. 2*), but the negative sign for the VCD at that frequency is correct. Below 1075 cm^{-1}, noise is introduced due to the cutoff from the CaF_2 windows. Only small changes are observed in the five IR and VCD solution spectra of **1**, and these correlate with band sharpening as the temperature decreases (*Fig. 3*). These nearly constant VCD and IR patterns are indicative of an equilibrium established when the sample is dissolved at 5°, which does not change over the temperature range and time period of the measurements.

In solution, the single stereoisomer found in the single crystal can undergo the conformational changes shown in *Scheme 3*, which include twisting of the biphenyl from (*P*)- to (*M*)-configuration (→**3**), rotation of the dihydrooxazole ring from an OH···N to an OH···O H-bonding orientation (→**2** or **4**) and three possible orienta-

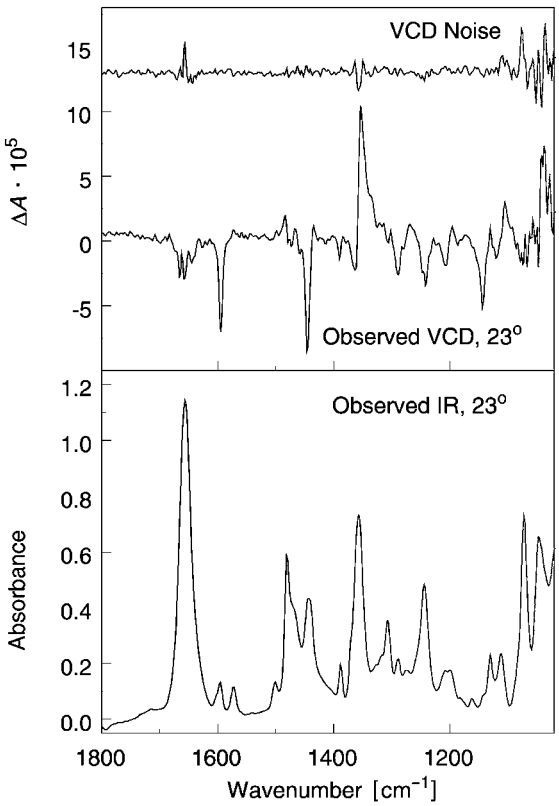

Fig. 2. *Observed IR* (lower frame) *and VCD* (upper frame) *spectra of (*P,S*)-***1*** in $CDCl_3$ solution at 23°.* 20-μm CaF_2 cell, 4 cm^{-1} resolution, 1 h collection time for sample and solvent, instrument optimized at 1400 cm^{-1}. The uppermost trace is the VCD noise.

tions of the isopropyl group (**a**–**c**), which produces a total of twelve conformations stabilized by intramolecular H-bonding. Calculations of the optimized geometry and of IR and VCD spectra were carried out at the DFT (B3LYP functional/6-31G(d) basis set) level for all twelve possibilities. The relative energies and geometric parameters for the optimized structures are compiled in *Table 1*. The optimized structures for six of the conformers are shown in *Fig. 4*.

In *Fig. 5*, the observed spectra for **1** in $CDCl_3$ at 23° and for solid (*P,S*)-**1** in a nujol oil mull are compared with the calculated spectrum for the (gas-phase) molecule **1a** in the crystal conformation. Differences between the observed mull spectra and the calculated spectra for the crystal conformation can be attributed to two possible factors. One is the effect of particle size on the VCD spectrum due to scattering of the IR radiation. Scattering is most pronounced when the average particle size exceeds the wavelength of the IR radiation. This leads to spectroscopic artefacts associated with the sign and shape of VCD and IR Bands. IR bands have a steep high-frequency side and a long-wavelength tail. Since the IR bands are fairly symmetric, it can be assumed that IR and VCD artefacts due to scattering from particles is not significant. A second factor is

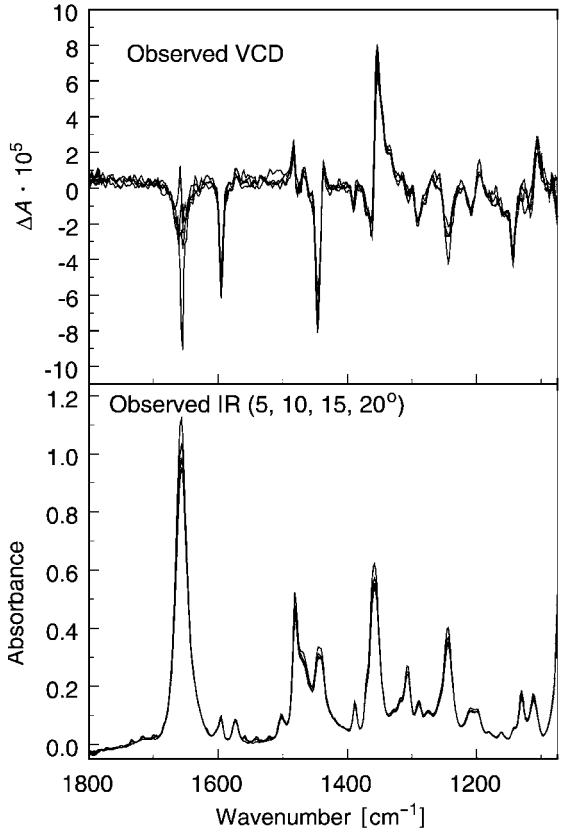

Fig. 3. *Overlay of IR* (lower frame) *and VCD* (upper frame) *spectra of* (P,S)-**1** *measured at 5, 10, 15, and 20°*. 20-μm CaF_2 cell, 4 cm^{-1} resolution, 1 h collection time for sample and solvent at each temperature, instrument optimized at 1400 cm^{-1}.

Table 1. *Relative Energies, Relative* Boltzmann P*opulations, Hydrogen-Bonding Properties and Dihedral Angles for Twelve Intramolecularly Hydrogen-Bonded Conformers of* **1** (see *Scheme 3*). Energies are relative to the lowest energy conformer in each set of three isopropyl group rotamers **a**–**c**.

	Rel. energy [kcal/mol]	*Boltzmann* population	H–C(15)–C(18)–H[a]) Dihedral [deg]	C(8)–C(7)–C(1)–C(2)[a]) Dihedral [deg]	H-Bond length [Å]	X–O–H Angle [deg]
(*P*,4*S*); OH···N: **1a**	0.193	0.382	–67	93	1.91	169
b	0.0	0.533	177	95	1.92	170
c	1.085	0.084	61	91	1.94	168
(*P*,4*S*); OH···O: **2a**	0.406	0.263	–66	99	2.01	163
b	0.0	0.525	–178	101	2.02	164
c	0.532	0.212	61	99	2.02	163
(*M*,4*S*); OH···N: **3a**	0.0	0.461	–72	–94	1.88	174
b	0.035	0.434	177	–96	1.92	173
c	0.732	0.105	55	–91	1.91	168
(*M*,4*S*); OH···O: **4a**	0.655	0.207	–69	–101	2.02	164
b	0.0	0.630	179	–99	2.01	163
c	0.796	0.163	57	–100	2.02	163

[a]) Arbitrary numbering according to *Fig. 1*.

Scheme 3

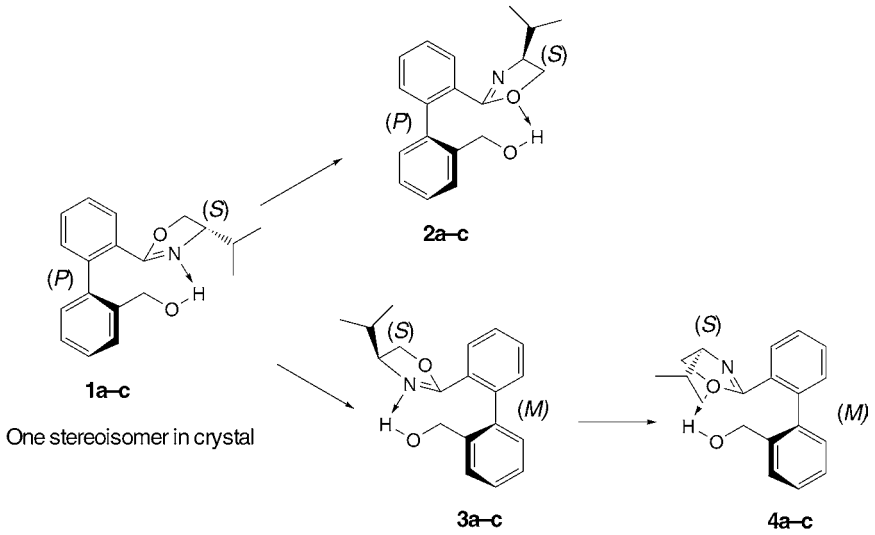

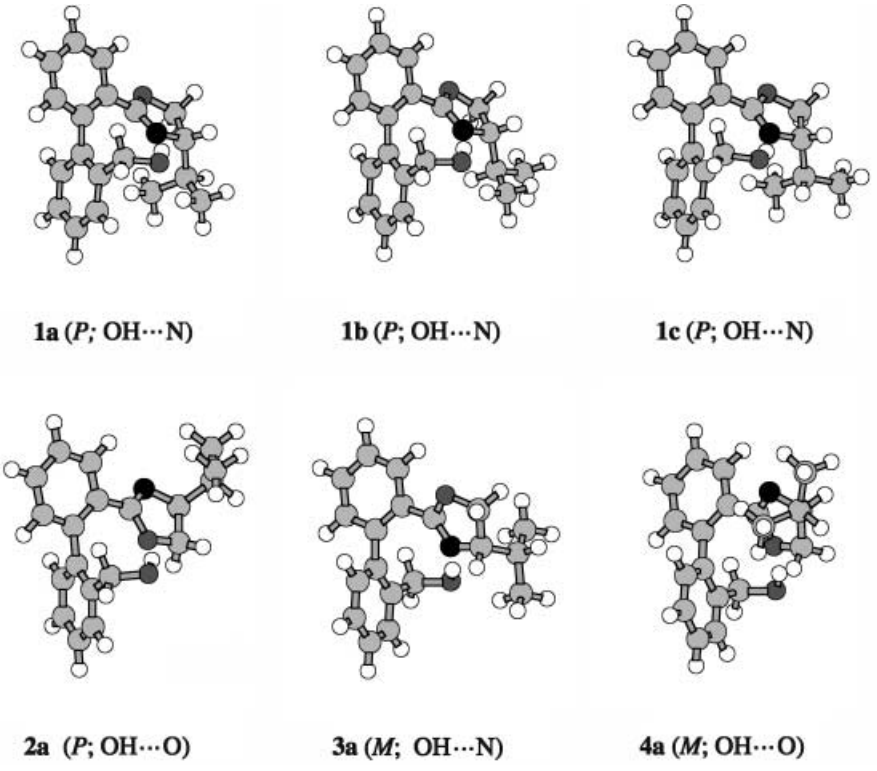

Fig. 4. *Calculated optimized geometries of* **1** *with* (P)*- or* (M)*-configuration, OH···N or OH···O hydrogen bonding, and isopropyl-group rotamers* (H–C(15)–C(18)–H dihedral angle: *ca.* –60° for **a**; *ca.* 180° for **b**, and *ca.* 60° for **c**)

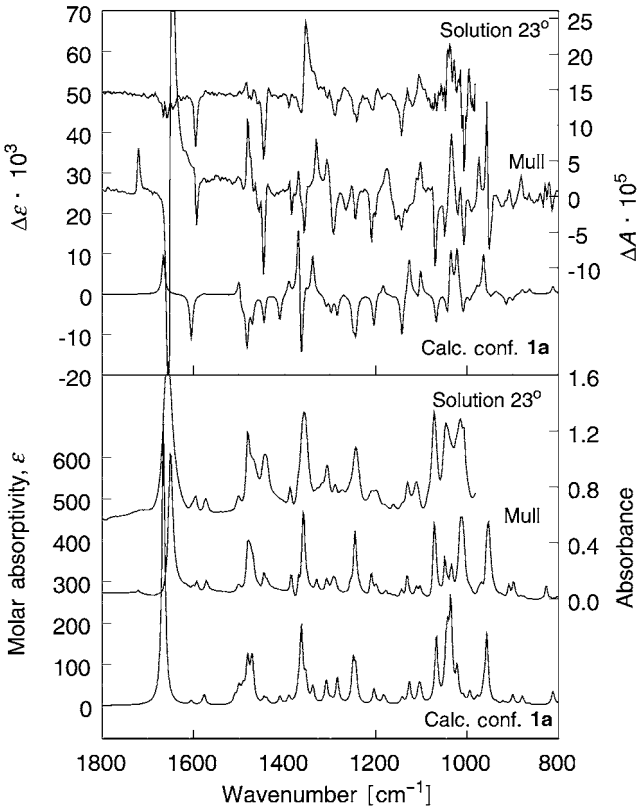

Fig. 5. *Comparison of IR* (lower frame) *and VCD* (upper frame) *spectra of* (P,S)-**1** *measured in* $CDCl_3$ *solution, as a solid mull in nujol oil* (right axes) *and calculated for crystal conformation* **1a** (left axes)

the absence of intermolecular interactions in the calculation, which is for an isolated molecule. In our experience, in only a few cases do observed VCD spectra for solids agree closely with the calculated spectra for an isolated molecule in the crystal conformation. In the case of this biphenyl molecule **1**, many VCD features of the mull spectrum are reproduced in the calculated spectrum, and the differences correlate with regions in which the observed and calculated IR spectra also differ. Differences are also noted between the mull and solution spectra of **1**, notably the large increase in IR intensity and negative VCD intensity at 1450 cm^{-1}, and the increase in positive VCD intensity at 1353 cm^{-1} in going from mull to solution. In addition, although a strong correlation between the observed solution VCD spectrum and that calculated for crystal conformation **1a** is noted below 1300 cm^{-1}, the correlation degrades for bands above 1300 cm^{-1}, and the feature at 1662 cm^{-1} in the calculated VCD spectrum is positive for **1a** but negative for all the solution spectra.

In the following analysis comparing observed and calculated intensities as well as frequencies, the observed spectra were converted to molar absorptivity units. Because of the small amount of sample and solvent, and some evaporation during the act of

placing the sample in the demountable *BioCell*, the concentration is not accurately known. The observed IR intensity was, therefore, scaled to be comparable with that calculated, and that same scaling factor was used for the observed VCD intensity. To identify other conformations present in solution, we first considered rotation of the isopropyl group. In *Fig. 6*, the solution spectra (23°) are compared with those calculated for conformers **1a**–**c** (which differ only in the orientation of the isopropyl group). Rotation of the isopropyl group has a large effect on the calculated VCD spectrum. In particular, the strong correlation in the 1175–1075 cm^{-1} region between the experimental and calculated VCD bands for conformer **1a** is not present in the calculated spectra for **1b** and **1c** or the *Boltzmann*-population-weighted composite spectra for **1a**–**c**. These data suggest that the orientation with the H–C(15)–C(18)–H dihedral angle *ca.* −67° is the most stable in solution, in contrast to that obtained from the calculation for the isolated molecule (*cf. Table 1 and Fig. 1*).

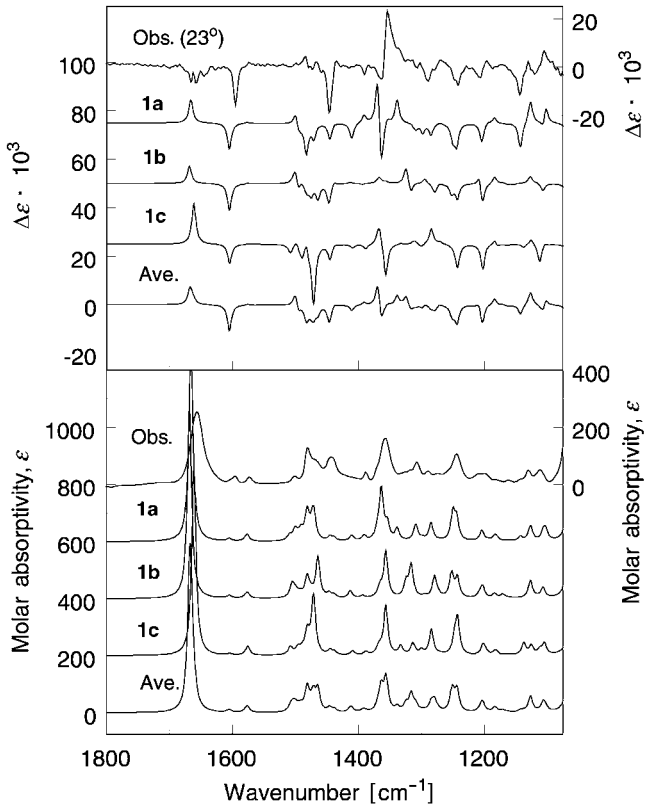

Fig. 6. *Comparison of IR* (lower frame) *and VCD* (upper frame) *spectra of (*P,S*)-***1** *observed for* $CDCl_3$ *solution at 23°* (right axes) *and calculated for conformers* **1a**–**c**, *and for the* Boltzmann-*population-weighted average of* **1a**–**c** (Ave.) (left axes, offset for clarity)

We next considered the effect of the $(P) \rightarrow (M)$ biphenyl twist and a 180° rotation of the dihydrooxazole ring to change the H-bonding interaction from OH···N to

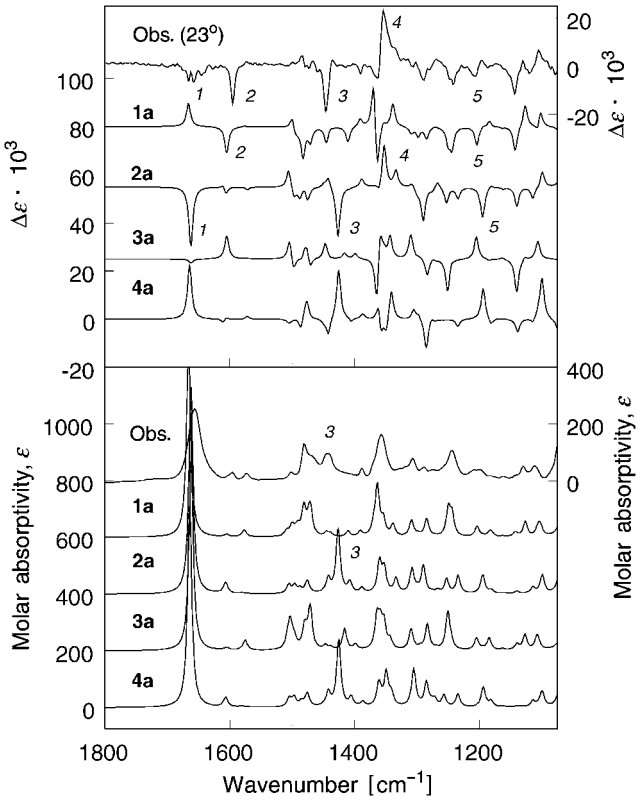

Fig. 7. *Comparison of IR* (lower frame) *and VCD* (upper frame) *spectra of* (P,S)-**1** *observed for* $CDCl_3$ *solution at 23°* (right axes) *and calculated for conformers* **1a**, **2a**, **3a** *and* **4a** (left axes, offset for clarity)

OH···O, while maintaining H–C(15)–C(18)–H[1]) *ca.* −70°: conformers **1a** (*P*; OH···N), **2a** (*P*; OH···O), **3a** (*M*; OH···N), and **4a** (*M*; OH···O) (*cf. Fig. 4*). The comparison of the calculated results for these four conformers with the experimental spectra is shown in *Fig. 7*, where five characteristic bands are labeled *1–5*. The dominant vibrational motion giving rise to each band is obtained by animating the calculated normal modes. *Band 1* (1660 cm^{-1}; predominantly ring C=N stretch) is negative only for conformer **2a** (*P*; OH···O H-bonding). *Band 2* (*ca.* 1600 cm^{-1}; biphenyl stretch coupled to C=N stretch) shows appreciable negative VCD intensity only for conformer **1a** (*P*; OH···N H-bonding). The IR intensity for *Band 3* (1444 cm^{-1} observed; 1425 cm^{-1} calculated for **2a** and **4a**) correlates with the orientation in which the OH···O H-bond is present; the observed intense negative VCD intensity for *Band 3*, which involves *trans* H–C–O–H deformation, is reproduced only for conformer **2a**. The positive VCD intensity for *Band 4* (1350 cm^{-1}, several modes involving the CH_2-wag of the CH_2OH and oxazole groups, and methine deformation) correlates with the VCD features calculated for conformer

[1]) Arbitrary numbering according to *Fig. 1*; for the systematic name, see *Exper. Part.*

2a. The negative VCD for *Band 5* (*ca.* 1200 cm^{-1}) is found only for the (*P*)-configuration conformers **1a** and **2a** (CH_2 twist and COH deformation of the CH_2OH group). Features of the opposite sign compared with the experiment are found, corresponding to *Bands 1*, *2*, *3*, and *5* for the (*M*)-configuration conformers **3a** and **4a**. Comparisons among the calculated spectra for all twelve conformers (**2b**, **2c**, **3b**, **3c**, **4b**, and **4c** not shown) revealed that the signs for *Bands 1*, *2*, *3*, and *5* change from (*P*)- to (*M*) configuration, but not on rotation of the isopropyl group.

In summary, analysis of the observed and calculated IR and VCD spectra identified *Band 2* as a marker for the (*P*)-configuration with OH ··· N H-bonding, as found in the crystal structure determination, and *Bands 1*, *3*, and *4* as markers for an additional conformer in solution with the (*P*)-configuration and OH ··· O H-bonding. *Band 5* is also a marker for the (*P*)-configuration. The VCD bands between 1175 and 1075 cm^{-1} serve as markers for the isopropyl-group orientation. An overall excellent fit between the observed and calculated spectra is obtained with a mixture of 20% of conformer **1a** and 80% of conformer **2a**, as shown in *Fig. 8*.

Examination of space-filling models for **1** suggests fairly free rotation of the dihydrooxazole group (**1a** → **2a**), but severe steric interference between the phenyl and

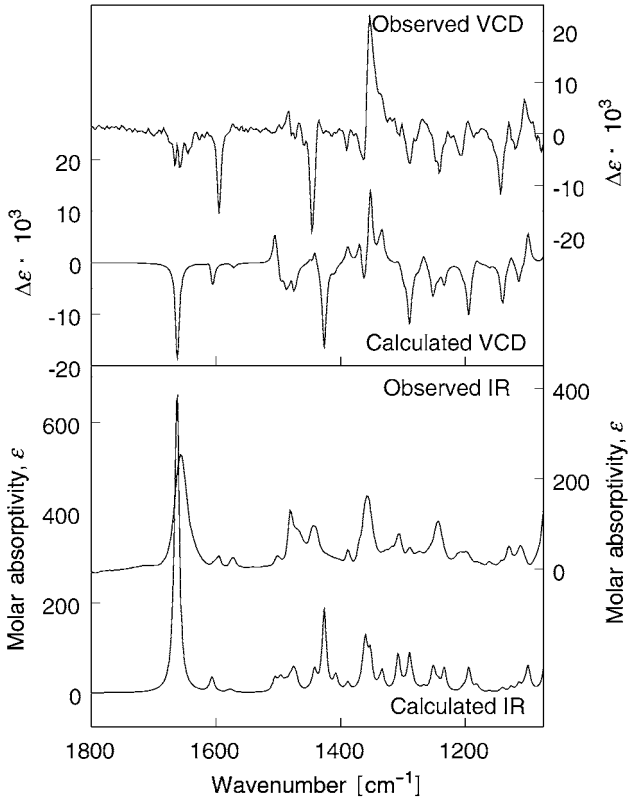

Fig. 8. *Comparison of IR* (lower frame) *and VCD* (upper frame) *spectra of* (P,S)-**1** *observed for* $CDCl_3$ *solution at 23°* (right axes) *and calculated for a mixture of conformers* **1a** (20%) *and* **2a** (80%) (left axes, offset for clarity)

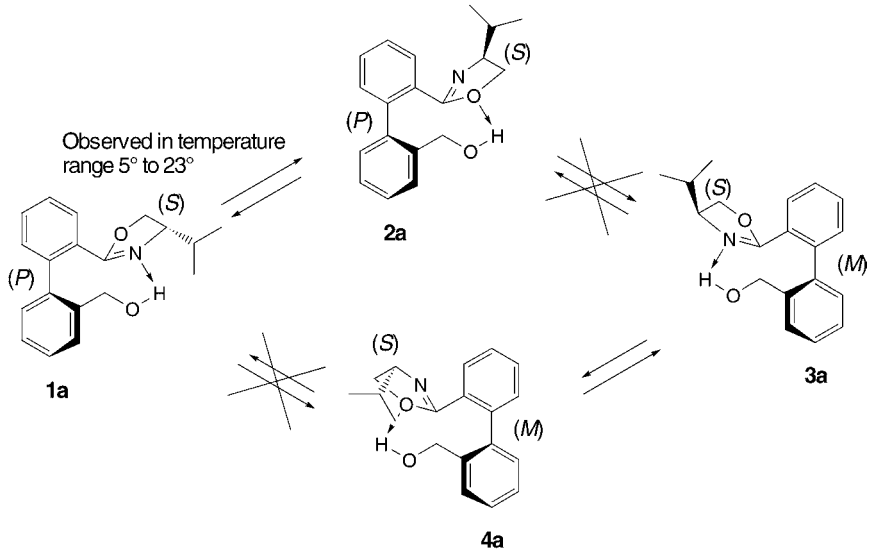

Fig. 9. *The two rotamers* **1a** *and* **2a** *of* (P,S)-**1** *observed by VCD measurements in* $CDCl_3$ *in a temperature range between 5° and 23°*. No evidence was found for a rotation of the chiral axis in the 1,1′-biphenyl moiety.

substituted dihydrooxazole moieties for $(P)\rightarrow(M)$ rotation of the 1,1′-biphenyl (*cf. Scheme 3*), consistent with the analysis described above, as illustrated in *Fig. 9*.

3. Conclusions. – This VCD investigation showed that dissolution of solid (*P*)-2′-[(4*S*)-4,5-dihydro-4-(1-methylethyl)oxazol-2-yl][1,1′-biphenyl]-2-methanol ((*P,S*)-**1**), which, in the crystalline form, has an OH···N H-bonded conformation with an isopropyl group orientation of H–C(15)–C(18)–H *ca.* −70°, in $CDCl_3$ solution at 5°, results in rapid equilibration of the orientation of the dihydrooxazole group but in no rotation of the isopropyl group or conversion from the (*P*)- to (*M*)-configuration. This compound, thus, exhibits an unexpected stability to atropisomerism. We are extending this investigation to 1,1′-biphenyl molecules with different '*peri*' substituents and with additional 6,6′-dimethyl substitution, which will be reported separately.

Experimental Part

General. All used solvents were distilled under N_2 prior to use. Methyl 2′-[(4*S*)-4,5-dihydro-4-(1-methylethyl)oxazol-2-yl][1,1′-biphenyl]-2′-carboxylate was synthesized in three steps from racemic [1,1′-biphenyl]-2,2′-dicarboxylic anhydride [15][16]. M.p.: apparatus constructed and assembled by *K. Hochreutener*, University of Zurich. Optical rotation: *Perkin-Elmer MC-941* polarimeter. CD: *Jasco J-715* spectropolarimeter; λ in nm ($\Delta\varepsilon$). UV: *Perkin-Elmer Lambda 19* spectrometer; λ_{max} in nm (log ε). IR: *Perkin-Elmer Spectrum-One* spectrometer, $\tilde{\nu}$ in cm^{-1}. ^{1}H- and ^{13}C-NMR: *Bruker ARX-300* spectrometer; δ in ppm rel. to the internal (Standard $SiMe_4$ = 0 ppm), *J* in Hz. Spectroscopic VCD measurements: All IR and VCD spectra were measured with a modified *Chiralir VCD* spectrometer (*BioTools, Inc.*) at 4 cm^{-1} resolution, with the instrument optimized at 1400 cm^{-1}. The IR and VCD spectra of (*P,S*)-**1** were obtained for the solid as a mull in nujol oil. A solution of (*P,S*)-**1** in $CDCl_3$ (*ca.* 10 mg/50 µl) was then prepared in a cold room at 5°, transferred to a 20-µm-path-length CaF_2 *BioCell*, provided by *BioTools, Inc.*, and then placed in a temp. control unit (TempCon from *BioTools*, Inc.), maintaining the low temp. during these transfers. IR and VCD spectra were measured at 5, 10,

15, and 20°, with a 1-h measurement time for sample and solvent. The sample was then held at r.t. (23°) overnight, and the r.t. spectrum obtained.

Calculations. The twelve possible conformer models were built with *HyperChem* software (*Hypercube, Inc.*, Gainsville, FL), and the geometries optimized with 'Gaussian 98' [17] at the DFT level with B3LYP functional and 6-31G* basis set. The vibrational frequencies and IR and VCD intensities were calculated with 'Gaussian 98' at the same DFT level, with the magnetic-field-perturbation [18] method for VCD incorporated into 'Gaussian 98', which utilizes gauge-invariant atomic orbitals [19][20]. The frequencies were scaled by 0.97, and the intensities were converted to Lorentzian bands with 4-cm^{-1} half-width for comparison with experiment.

*Formation of (*P,S*)-***1*** (last synthetic step).* An ice-cold soln. of methyl 2′-[(4*S*)-4,5-dihydro-4-(1-methylethyl)oxazol-2-yl][1,1′-biphenyl]-2-carboxylate (12.92 g, 40.0 mmol) in Et_2O (250 ml) was treated with $LiBH_4$ (1.31 g, 60.0 mmol) followed by the addition of MeOH (2.43 ml, 60.0 mmol). The mixture was stirred at r.t. overnight. Under cooling, the suspension was quenched with 1M NaOH (200 ml). The aq. phase was then extracted with ^{t}BuOMe, the org. phase dried (Na_2SO_4) and evaporated, and the residue purified by column chromatography (^{t}BuOMe/hexane 1:2, 1% EtN_3): 6.48 g (55%) of (*P,S*)-**1** and 3.42 g (28%) of (*P,S*)-**1** · BH_3. To remove the BH_3, **1** · BH_3 was taken up in toluene and warmed at 40° for 4 h in the presence of 1,4-diazobicyclo[2.2.2]octane (DABCO; 1.35 g, 12 mmol). After purification by column chromatography (^{t}BuOMe/hexane 1:2, 1% Et_3N), another product fraction of (*P,S*)-**1** (2.39 g, 77%) was obtained as a white solid (overall yield of (*P,S*)-**1**: 9.41 g, 80%). A sample (1.10 g, 3.73 mmol) of (*P,S*)-**1** was recrystallized from ^{t}BuOMe/hexane to yield 0.97 g (88%; total yield after crystallization, 66%).

*(*P*)-2′-[(4*S*)-4,5-Dihydro-4-(1-methylethyl)oxazol-2-yl][1,1′-biphenyl]-2-methanol* (*P,S*)-(**1**): M.p. 63–66°. R_f (^{t}BuOMe/hexane 3:1) 0.52. $[\alpha]_D^{20} = -38°$ (EtOH, $c = 1.01$). CD (MeCN, $c = 2.20 \cdot 10^{-5}$): 214 (−4.1), 249 (2.0). UV (MeCN, $c = 2.20 \cdot 10^{-5}$): 194 (5.4), 197 (sh, 5.2), 202 (4.6), 205 (sh, 4.1), 248 (sh, 0.7). IR (KBr): 3689*w*, 3210*m*, 3066*m*, 3027*m*, 2998*s*, 2964*vs*, 2933*s*, 2908*s*, 2875*s*, 1658*vs*, 1598*m*, 1574*w*, 1502*w*, 1481*s*, 1441*m*, 1389*w*, 1357*s*, 1307*m*, 1289*w*, 1245*s*, 1208*m*, 1131*m*, 1112*w*, 1072*s*, 1047*m*, 1008*s*, 961*s*, 910*w*. ^{1}H-NMR (300 MHz, $CDCl_3$; 2 rotamers A/B 2.8:1): 7.71–7.66 (*m*, 1 arom. H, A and B); 7.52–7.19 (*m*, 6 arom. H, A and B); 7.01 (*d*, $^3J = 7.5$, 1 arom. H, B); 6.98 (*d*, $^3J = 7.6$, 1 arom. H, A); 5.96 (*dd*, $^3J = 9.2$, 1.2, OH, A); 5.26 (*dd*, $^3J = 9.0$, 1.9, OH, B); 4.47 (*dd*, $J_{AB} = 10.7$, $^4J = 0.8$, CH_2, A and B); 4.34–4.14 (*m*, 4 H); 3.98–3.78 (*m*, 3 H, 2A and B); 3.65 (*m*, 1 H, B); 1.67 (*oct*, $^3J = 6.7$, Me_2CH, B); 1.27 (*oct*, $^3J = 6.7$, Me_2CH, A); 0.85, 0.77 (2 *d*, $^3J = 6.8$, 6.8 Me_2CH, B); 0.56, 0.43 (2 *d*, $^3J = 6.9$, 6.9 Me_2CH, A). ^{1}H-NMR (−40°, A/B 3.0:1): 7.72–7.68 (*m*, 1 arom. H, A and B); 7.51–7.21 (*m*, 6 arom. H, A and B); 7.01 (*dd*, $^3J = 7.5$, $^4J = 1.4$, 1 arom. H, B); 6.98 (*dd*, $^3J = 7.6$, $^4J = 1.3$, 1 arom. H, A); 5.8 (br. *s*, OH); 5.2 (br. *s*, OH); 4.47 (*dd*, $J_{AB} = 10.8$, $^4J = 0.8$, CH_2); 4.34–4.15 (*m*, 4 H); 3.98–3.83 (*m*, 4 H); 3.72–3.62 (*m*, 2 H); 1.70 (*oct.*, $^3J = 6.7$, Me_2CH, B); 1.25 (*oct.*, $^3J = 6.7$, Me_2CH, A); 0.84, 0.76 (2 *d*, $^3J = 6.8$, 6.8, Me_2CH, B); 0.54, 0.40 (2 *d*, $^3J = 6.9$, 6.9, Me_2CH, A). ^{13}C-NMR (75 MHz, $CDCl_3$): 164.2; 163.9; 141.3; 141.0; 140.9; 140.4; 139.3; 139.0; 130.5; 130.4; 130.0; 129.9; 129.8, 129.5; 128.9; 128.7; 128.6; 128.5, 128.0; 127.5; 127.3; 127.0, 126.9; 72.4; 72.2; 70.4, 70.3; 63.6; 63.4; 32.6; 32.3; 18.5; 18.3; 18.1; 17.4. CI-MS (NH_3): 297 (20), 296 (100, $[M+H]^+$), 294 (9). Anal. calc. for $C_{19}H_{21}NO_2$ (295.38): C 77.26, H 7.17, N 4.74, O 10.83; found: C 77.09, H 7.05, N 4.58.

X-Ray Crystal-Structure Determination of (P,S)-**1** (see *Table 2* and *Fig. 1*)[2]). All measurements were conducted on a *Nonius-KappaCCD* area-detector diffractometer [21] with graphite-monochromated Mo$K\alpha$ radiation (λ 0.71073 Å) and an *Oxford-Cryosystems Cryostream-700* cooler. Data reduction was performed with 'HKL Denzo' and 'Scalepack' [22]. The intensities were corrected for *Lorentz* and polarization effects but not for absorption. Equivalent reflections other than *Friedel* pairs were merged. The data collection and refinement parameters are given in *Table 2*, and a view of the molecule is shown in *Fig. 1*. The structure was solved by direct methods with 'SHELXS97' [23]. The non-H-atoms were refined anisotropically. The hydroxy H-atom was placed in the position indicated by a difference electron-density map, and its position was allowed to refine together with an isotropic displacement parameter. All remaining H-atoms were fixed in geometrically calculated positions (d(C–H) = 0.95 Å), and each was assigned a fixed isotropic displacement parameter with a value equal to 1.2 *U*eq of its parent C-atom. The absolute configuration could not be determined crystallographically due to the absence of significant anomalous scattering in the compound. Instead, the enantiomer used in the refinement was based on the known (*S*)-configuration of the chiral center in the oxazole moiety. Refinement of the structure was carried out on *F* by full-matrix least-squares procedures that minimized the

---

[2]) CCDC-207612 contains the supplementary crystallographic data for this paper. These data can be obtained free of charge *via* www.ccdc.cam.ac.uk/conts/retrieving.html (or from the *Cambridge Crystallographic Data Centre*, 12 Union Road, Cambridge CB2 1EZ, UK; fax: +44 1223 336033; e-mail: deposit@ccdc.cam.ac.uk).

function $\Sigma w(|F_o| - |F_c|)^2$. A correction for secondary extinction was applied. Neutral-atom scattering factors for non-H-atoms were taken from [24a] and the scattering factors for H-atoms from [25]. Anomalous dispersion effects were included in *Fc* [26]; the values for *f′* and *f″* were those of *Creagh* and *McAuley* [24b], and the values of the mass-attenuation coefficients were those of [24c]. All calculations were performed with the 'teXsan' crystallographic software package [27], and *Fig. 1* was drawn with 'ORTEPII' [28].

Table 2. *Crystallographic Data of Compound (*P,S*)*-**1**

Crystallized from	^{t}BuOMe/hexane	$F(000)$	632
Empirical formula	$C_{19}H_{21}NO_2$	D_x [g cm^{-3}]	1.185
M_r	295.38	μ(Mo $K\alpha$) [mm^{-1}]	0.0763
Crystal color, habit	colourless, prism	2θ(max) [°]	60
Crystal dimensions [mm]	$0.20 \times 0.30 \times 0.30$	Total reflections measured	14790
Temperature [K]	298 (1)	Symmetry-independent reflections	4467
Crystal system	orthorhombic	R_{int}	0.052
Space group	$P2_12_12_1$ (#19)	Reflections used ($I > 2\sigma(I)$)	3344
Z	4	Parameters refined	204
Reflections for cell determination	2538	Final R	0.0459
2θ Range for cell determination [°]	5–69	wR	0.0475
Unit cell parameters a [Å]	8.8684 (2)	Weights: p in $w = [\sigma^2(F_o) + (pF_o)^2]^{-1}$	0.010
b [Å]	9.3178 (2)	Goodness of fit	1.879
c [Å]	20.0320 (4)	Secondary extinction coefficient	1.5 (2) $\times 10^{-5}$
V [Å^3]	1655.32 (6)	Final Δ_{max}/σ	0.0004
		$\Delta\rho$ (max; min) [e Å^{-3}]	0.16; −0.13

REFERENCES

[1] R. Adams, H. C. Yuan, *Chem. Rev.* **1933**, *12*, 261.
[2] H. Hillemann, *Angew. Chem.* **1937**, *50*, 435.
[3] F. H. Westheimer, *J. Chem. Phys.* **1947**, *15*, 252.
[4] J. W. Brooks, M. M. Harris, K. E. Howlett, *J. Chem. Soc.* **1957**, 2380.
[5] D. M. Hall, M. M. Harris, *J. Chem. Soc.* **1960**, 490.
[6] W. Theilacker, R. Hopps, *Chem. Ber.* **1959**, *92*, 2293.
[7] G. Bringmann, D. Menche, *Angew. Chem. Int. Ed.* **2001**, *40*, 1687.
[8] G. Bringmann, D. Menche, *Acc. Chem. Res.* **2001**, *34*, 615.
[9] K. Mislow, H. B. Hopps, *J. Am. Chem. Soc.* **1962**, *84*, 3018.
[10] L. A. Nafie, T. B. Freedman, in 'Circular Dichroism', 2nd edn., Eds. K. Nakanishi, N. Berova, and R. Woody, Wiley-VCH, New York, 2000, p. 97.
[11] L. A. Nafie, T. B. Freedman, in 'Infrared and Raman Spectroscopy of Biological Materials', Eds. H.-U. Gremlich and B. Yan, Marcel Dekker, Inc., New York, 2000, p. 15.
[12] P. J. Stephens, F. J. Devlin, *Chirality* **2000**, *12*, 172.
[13] T. B. Freedman, X. Cao, R. V. Oliveira, Q. B. Cass, L. A. Nafie, *Chirality* **2003**, *15*, 196.
[14] T. B. Freedman, X. Cao, A. Rajca, H. Wang, L. A. Nafie, *J. Phys. Chem. A*, submitted.
[15] M. Kalbermatter, A. J. Rippert, in preparation; M. Kalbermatter, Ph. D. Thesis, University of Zürich, 2002.
[16] R. Röhrkasten, R. P. Kreher, *Chem. Ber.* **1991**, *124*, 2085.
[17] M. J. Frisch, G. W. Trucks, H. B. Schlegel, G. E. Scuseria, M. A. Robb, J. R. Cheeseman, V. G. Zakrzewski, J. A. Montgomery Jr., R. E. Stratmann, J. C. Burant, S. Dapprich, J. M. Millam, A. D. Daniels, K. N. Kudin, M. C. Strain, O. Farkas, J. Tomasi, V. Barone, M. Cossi, R. Cammi, B. Mennucci, C. Pomelli, C. Adamo, S. Clifford, J. Ochterski, G. A. Petersson, P. Y. Ayala, Q. Cui, K. Morokuma, D. K. Malick, A. D. Rabuck, K. Raghavachari, J. B. Foresman, J. Cioslowski, J. V. Ortiz, B. B. Stefanov, G. Liu, A. Liashenko, P. Piskorz, I. Komaromi, R. Gomperts, R. L. Martin, D. J. Fox, T. Keith, M. A. Al-Laham, C. Y. Peng, A. Nanayakkara, C. Gonzalez, M. Challacombe, P. M. W. Gill, B. Johnson, W. Chen, M. W. Wong, J. L. Andres, C. Gonzalez, M. Head-Gordon, E. S. Replogle, J. A. Pople, 'Gaussian 98, A.9', Gaussian, Inc., Pittsburgh, PA, 1998.
[18] P. J. Stephens, F. J. Devlin, C. F. Chabalowski, M. J. Frisch, *J. Phys. Chem.* **1994**, *98*, 11623.

[19] K. L. Bak, F. J. Devlin, C. S. Ashvar, P. R. Taylor, M. J. Frisch, P. J. Stephens, *J. Phys. Chem.* **1995**, *99*, 14918.
[20] L. A. Nafie, *J. Chem. Phys.* **1992**, *96*, 5687.
[21] R. Hooft, 'KappaCCD Collect Software', Nonius BV, Delft, The Netherlands, 1999.
[22] Z. Otwinowski, W. Minor, in 'Methods in Enzymology', Vol. 276, 'Macromolecular Crystallography', Part A, Eds. C. W. Carter Jr., and R. M. Sweet, Academic Press, New York, 1997, p. 307.
[23] G. M. Sheldrick, 'SHELXS97, Program for the Solution of Crystal Structures', University of Göttingen, Germany, 1997.
[24] a) E. N. Maslen, A. G. Fox, M. A. O'Keefe, in 'International Tables for Crystallography', Ed. A. J. C. Wilson, Kluwer Academic Publishers, Dordrecht, 1992, Vol. C, Table 6.1.1.1, p. 477; b) D. C. Creagh, W. J. McAuley, in 'International Tables for Crystallography', Ed. A. J. C. McAuley, Vol. C, Table 4.2.6.8, p. 219; c) D. C. Creagh, J. H. Hubbell, in 'International Tables for Crystallography', Ed. A. J. C. McAuley, Vol. C, Table 4.2.4.3, p. 200.
[25] R. F. Stewart, E. R. Davidson, W. T. Simpson, *J. Chem. Phys.* **1965**, *42*, 3175.
[26] J. A. Ibers, W. C. Hamilton, *Acta Crystallogr.* **1964**, *17*, 781.
[27] 'teXsan: Single Crystal Structure Analysis Software', Version 1.10, Molecular Structure Corporation, The Woodlands, Texas, 1999.
[28] C. K. Johnson, 'ORTEPII'. Report ORNL-5138, Oak Ridge National Laboratory, Oak Ridge, Tennessee, 1976.

Received April 17, 2003